Chinese Chemical Letters 35 (2024) 109100

Contents lists available at ScienceDirect

Chinese Chemical Letters

journal homepage: www.elsevier.com/locate/cclet

Niduenes A–F, six functionalized sesterterpenoids with a pentacyclic 5/5/5/5/6 skeleton from endophytic fungus *Aspergillus nidulans*

Aimin Fu[1], Chunmei Chen[1], Qin Li[1], Nanjin Ding, Jiaxin Dong, Yu Chen, Mengsha Wei, Weiguang Sun*, Hucheng Zhu*, Yonghui Zhang*

Hubei Key Laboratory of Natural Medicinal Chemistry and Resource Evaluation, School of Pharmacy, Tongji Medical College, Huazhong University of Science and Technology, Wuhan 430030, China

ARTICLE INFO

Article history:
Received 21 July 2023
Revised 11 September 2023
Accepted 13 September 2023
Available online 16 September 2023

Keywords:
Aspergillus nidulans
Sesterterpenoids
Aromatic sesterterpenoids
Structure elucidation
Single-crystal X-ray diffraction
Biosynthetic pathways

ABSTRACT

Niduenes A–F (**1**–**6**), six novel sesterterpenoids with unprecedented 5/5/5/5/6 pentacyclic ring skeleton were isolated from endophytic fungus *Aspergillus nidulans*. Compounds **1** and **2** represent the first examples of aromatic pentacyclic sesterterpenoids. Their structures and configurations were elucidated by spectroscopic data and single-crystal X-ray diffraction analyses. Compound **4** demonstrated potent resensitization of SW620/AD300 cells to paclitaxel (PTX). Rhodamine 123 accumulation assay and docking analysis further support that **4** inhibitory the efflux function of P-glycoprotein (P-gp).

Sesterterpenoids, the smallest subgroup of the terpenoids, have been isolated from insects, marine organisms, higher plants, and fungi [1–6], and exhibited various pharmacological characteristics, such as anticancer [7], anti-inflammatory [8], antitubercular [9], antimicrobial activities [10], and anti-adipogenic activity [11]. Aromatization relatively rare occurs in sesterterpenoids, the first aromatic sesterterpenoid phorone A was isolated from a marine sponge *Phorbas* sp. in 2012 [12]. To date, more than 1300 sesterterpenoids with diverse carbon skeletons have been discovered [13], however, only eight of them possess aryl ring (Fig. S2), which were reported from the genera *Hippospongia* [14], *Phorbas* [12,15], *Clathria* [16], and *Stahlianthus* [17].

Fungal derived terpenoids have been widely study [18–22], we have isolated the first examples of hexacarbocyclic sesterterpenoids named niduterpenoids A and B from *Aspergillus nidulans* [23], and their uncommon skeleton and bioactive drawn our attention to dig deeply into the secondary metabolites of this strain. Herein, the isolation and structure elucidation of six sesterterpenoids possessing a 5/5/5/5/6 pentacarbocyclic ring system are presented. All structures and absolute configurations were elucidated by extensive spectroscopic analysis and single-crystal X-ray diffraction analysis. Compounds **1**–**6** (Fig. 1) represent a new type of sesterterpenoids possessing a 5/5/5/5/6 pentacarbocyclic ring system, and **1** and **2** were the first examples of aromatic pentacarbocyclic sesterterpenoids. Compound **4** demonstrated potent resensitization of SW620/AD300 cells to PTX by lowering the half maximal inhibitory concentration (IC_{50}) values of PTX up to 5.26-fold from 340 nmol/L to 1.79 μmol/L. Moreover, a possible biosynthetic pathway of these unusual terpenoid natural products is proposed.

Niduene A (**1**) was obtained as colorless crystals. The molecular ion peak at *m/z* 421.2718 (calcd. for $C_{26}H_{38}O_3Na^+$, 421.2719) verified its molecular formula with eight degrees of unsaturation. The infrared spectroscopy (IR) spectrum showed the presence of hydroxyl groups (3421 cm^{-1}) and aromatic ring (1622 and 1513 cm^{-1}). Its ^1H nuclear magnetic resonance (NMR) data (Table S1 in Supporting information) displayed signals characteristic of six methyl groups [δ_H 2.31 (s), 1.51 (s), 1.50 (s), 1.31 (s), 1.05 (d, *J*=7.1 Hz), and 1.02 (s)], one methoxy group (δ_H 2.98), one oxygenated methine group [δ_H 4.04 (dd, *J*=8.4, 5.4 Hz)], and two aromatic methines [δ_H 6.97 and 6.91 (both d, *J*=8.0 Hz)]. The ^{13}C and distortionless enhancement by polarization transfer (DEPT) NMR spectroscopic data (Table S2 in Supporting information) of **1** highlighted the presence of 26 carbon resonances, including six methyl, a methoxy group (δ_C 50.5), four methylenes, seven methines (two aromatics), eight nonprotonated carbons (four sp^2 hybrid and two oxygenated). The six sp^2 hybrid carbons accounted for three degrees of unsaturation, whereas the remaining unsaturated degrees

* Corresponding authors.
E-mail addresses: weiguangsun@hust.edu.cn (W. Sun), zhuhucheng@hust.edu.cn (H. Zhu), zhangyh@mails.tjmu.edu.cn (Y. Zhang).
[1] These authors contributed equally to this work.

https://doi.org/10.1016/j.cclet.2023.109100
1001-8417/

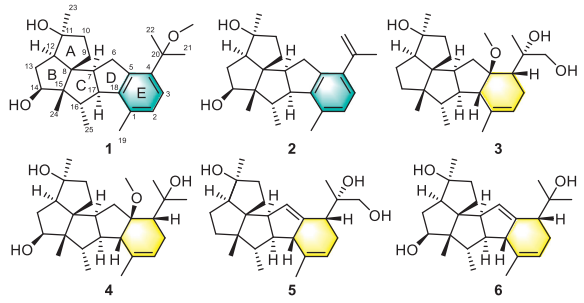

Fig. 1. Structures of compounds **1**–**6**.

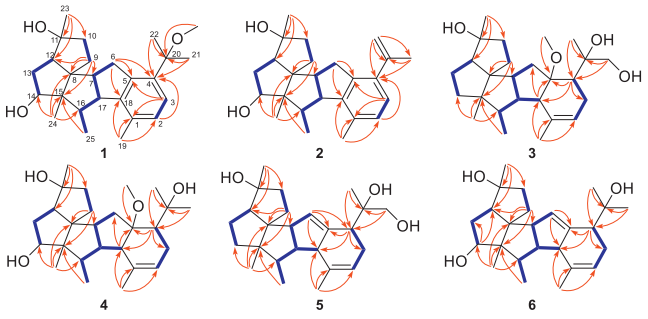

Fig. 2. Key ^{1}H–^{1}H COSY and key HMBC correlations of compounds **1**–**6**.

confirmed that **1** was a sesterterpenoid with a pentacyclic ring system.

The ^{1}H–^{1}H correlated spectroscopy (COSY) correlations of **1** (Fig. 2) revealed the presence of four independent spin systems: H-2/H-3, H_2–6/H-7/H-17/H-16/Me-25, H_2–9/H_2–10, and H-12/H_2–13/H-14. The heteronuclear multiple-bond correlation (HMBC) correlations (Fig. 2) from H_2–6 to C-5 and C-18, from H_2–9 to C-7, C-8, C-12, and C-15, from Me-23 to C-10, C-11, and C-12, and from Me-24 to C-8, C-14, C-15, and C-16 established the condensed nucleus of rings A–D that is similar to niduterpenoid A [23]. In addition, the HMBC correlations from H-2 to C-4, from H-3 to C-1 and C-5, from H_2–6 to C-4 and C-5, from Me-19 to C-1, C-2, and C-18 formed an aromatic ring (E-ring). Subsequently, the HMBC correlations from Me-21 and Me-22 to C-4 and C-20, from OMe-20 to C-20 indicated that a terminal 2-methoxyisopropyl group is attached to C-4. Finally, a detailed analysis of ^{1}H–^{1}H COSY, heteronuclear single quantum coherence (HSQC), and HMBC spectra established the planar structure of **1**, featuring a complex and rigid 5/5/5/5/6 pentacyclic skeleton.

The relative configuration of **1** was determined by analysis of the nuclear overhauser effect spectroscopy (NOESY) spectrum (Fig. S9 in Supporting information). The NOESY correlations of Me-23/H-12, H-12/H-7, H-7/H-17, H-7/H-9α, and H-17/H-14 revealed they were cofacial and arbitrarily were assigned to be α-oriented, which suggested a *cis*-fusion pattern for rings A and B. Moreover, *cis*-fused rings B/C and β-oriented of Me-24 and H-16 were consistent with the observed correlations of Me-24/H-9β and Me-24/H-16. The single crystal of **1** was fortunately obtained in MeOH/CH_2Cl_2/H_2O (64:32:4) at room temperature, the structure and absolute configuration of **1** were subsequently confirmed by single-crystal X-ray diffraction experiment using Cu Kα radiation (Fig. 3) with the Flack parameter of 0.11(7) (CCDC 2272298).

Niduene B (**2**) had a molecular formula of $C_{25}H_{34}O_2$, based on its high resolution electrospray ionization mass spectroscopy (HRESIMS) (*m/z* 389.2471 $[M+Na]^+$, calcd. 389.2457). The ^{1}H and ^{13}C NMR spectra of **2** were highly similar to these of **1**, except for the presence of a double bond (δ_C 146.1 and 114.6) and the absence of one methoxy group, which was supported

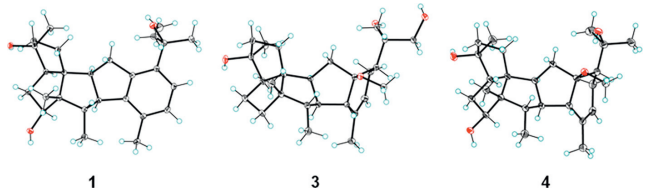

Fig. 3. ORTEP (Oak Ridge thermal ellipsoid plot) drawing of compounds **1**, **3**, and **4**.

by the HMBC correlations from H_2–22 and Me-21 to C-4 and C-20 (Fig. 2). The analysis of the NOESY spectrum (Fig. S3), correlations of Me-23/H-12, H-12/H-7, H-7/H-17, H-7/H-9α, and H-17/H-14 suggested **2** shared the same relative configuration with **1**, and the co-occurrence and similar specific rotation values of the two compounds ($[\alpha]_D^{20}$ +32 (*c* 0.1, MeOH) of **1**, $[\alpha]_D^{20}$ +32 (*c* 0.1, MeOH) of **2**) indicating their consistent absolute configurations.

Niduene C (**3**) was assigned to have the molecular formula of $C_{26}H_{42}O_4$, based on its HRESIMS (*m/z* 441.2970 $[M+Na]^+$, calcd. 441.2981), requiring six degrees of unsaturation. The NMR spectra of **3** were similar to these of **1**, the 1D NMR spectra and the degrees of unsaturation suggested that the aromatic ring (E-ring) was dearomatization. ^{1}H–^{1}H COSY correlations of H-2/H_2–3/H-4 and the HMBC correlations from H-4 to C-5 and C-18, and from Me-19 to C-1, C-2, and C-18 formed the E ring (Fig. 2). Furthermore, the HMBC correlations from H_2–21 and H_3–22 to C-4 and C-20 suggested that one of the *gem*–dimethyl groups was oxidized to hydroxymethyl. In addition, an oxygenated methine of C-14 in **1** was displaced by a methylene group (δ_C 37.4), which was deduced by the ^{1}H–^{1}H COSY correlations of H-12/H_2–13/H_2–14. Finally, the structure and the stereochemistry of **3** were confirmed by a single-crystal X-ray analysis with the refinement of Flack's parameter of 0.16(11) (Fig. 3).

Niduene D (**4**) was isolated as colorless crystals. It had a molecular formula of $C_{26}H_{42}O_4$ as disclosed by the $[M+Na]^+$ ion peak at *m/z* 441.2982 in the HRESIMS spectrum (calcd. for $C_{26}H_{42}O_4Na$, 441.2981), which was the same as that of **3**. Carefully compared the ^{1}H and ^{13}C NMR spectra of **4** and **3** suggested that **4** closely resembled **3**, differing from the methyl singlet (δ_H 1.29; δ_C 30.8) at C-21 and an oxygenated methine (δ_H 3.84 m; δ_C 77.4) at C-14. The HMBC signal from H-14 to C-12 and C-13, from Me-21 to C-4 and C-20, and COSY correlations of H-13/H-14 supported the structure. The relative configuration of **4** was determined by the NOESY spectrum analysis, the NOESY interaction between H-14 and H-17 suggested that H-14 was α-oriented. Furthermore, the complete structure and stereochemistry of **4** were also confirmed by a single-crystal X-ray diffraction experiment with the Flack parameter of 0.01(12).

The assign niduene E (**5**) was isolated as a white powder and the molecular formula of $C_{25}H_{38}O_3$ was deduced from the HRESIMS (*m/z* 409.2722 $[M+Na]^+$, calcd. 409.2719 for $C_{25}H_{38}O_3Na^+$), requiring seven degrees of unsaturation. The NMR spectra of **5** were highly similar to these of **3**, except for the presence of a trisubstituted double bond located at C-5 (δ_C 142.7) and C-6 (δ_C 121.3), which was supported by the ^{1}H–^{1}H COSY correlation (Fig. 2) of H-6/H-7, and the HMBC correlations from H-6 to C-4, C-5, and C-18 (Fig. 2). The relative configuration of **5** was determined by analysis of the NOESY spectrum, the correlations of Me-23/H-12, H-12/H-7, H-7/H-17 revealed the relative configuration of **5** was consistent with **1**.

Niduene F (**6**) gave the same molecular formula ($C_{25}H_{38}O_3$) as **5** determined by HEESIMS data (*m/z* 409.2720 $[M+Na]^+$, calcd. 409.2720 for $C_{25}H_{38}O_3Na^+$). Analysis of the NMR spectra (Tables S1 and S2) of **6** revealed the planar structure similar to that of **5**. Ac-

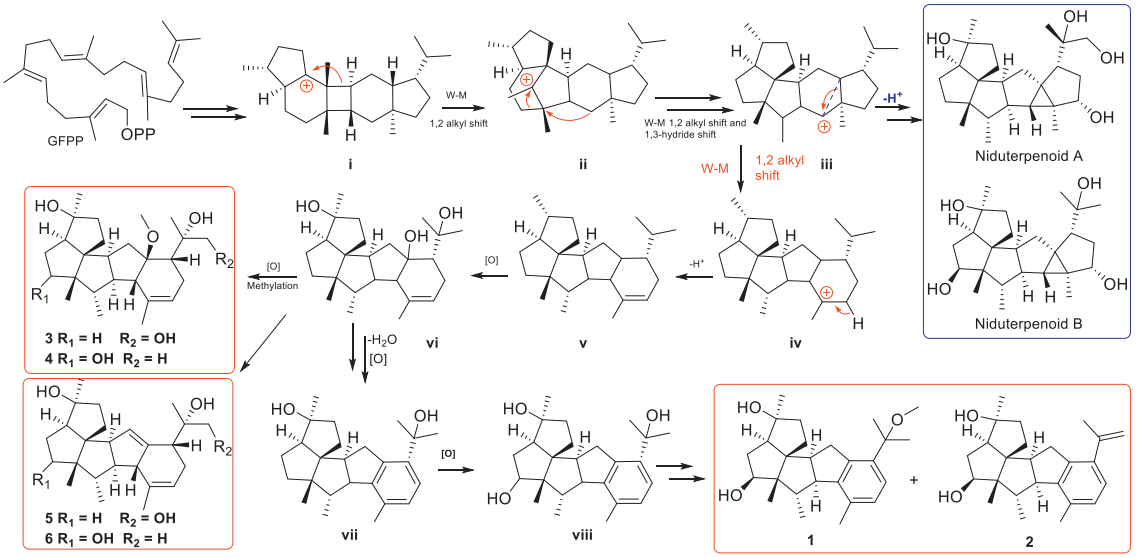

Scheme 1. Proposed biogenetic pathway of **1**–**6**.

cording to the ^{1}H–^{1}H COSY correlations of H_2–13/H-14, as well as the HMBC correlations from H-14 to C-13 and C-15, the methylene group at C-14 was replaced by an oxygenated methine. In addition, the key HMBC correlation of Me-21 with C-4 and the shielded signal of C-21 (δ_C 27.6) revealed the replacement of the oxygenated methylene group in **5** by a methyl group in **6**. The NOESY cross-peaks revealed the same relative configuration of **6** and **5**, and further comparison of the specific rotation values of **5** and **6** with **3** {$[\alpha]_D^{20}$ +55 (*c* 0.1, MeOH) of **5**, $[\alpha]_D^{20}$ +55 (*c* 0.1, MeOH) of **6** and $[\alpha]_D^{20}$ +40 (*c* 0.1, MeOH) of **3**} suggested their same absolute configurations.

To the best of our knowledge, niduenes A–F (**1**–**6**) represent the first examples of sesterterpenoids possessing a 5/5/5/5/6 pentacarbocyclic ring system, and **1** and **2** were the first aromatic pentacarbocyclic sesterterpenoids. To better understand these structures, a hypothetical biosynthetic pathway was proposed (Scheme 1). The initial head-to-tail cyclization of geranylfranesyl pyrophosphate (GFPP) and Wagner–Meerwein alkyl and hydride shift produces a 5/5/5/6/5 fuse ring intermediate **iii** [24,25], followed by Wagner–Meerwein alkyl shift to generate a 5/5/5/5/6 pentacyclic ring intermediate **iv**, subsequent oxidation and methylation reactions afford compounds **1**–**6**.

To evaluate the cellular toxicity of **1**–**6**, sorts of cell lines have been used to examine by cell counting kit-8 (CCK-8) assay, which was carried out with the previously reported method [26]. As shown in Table S3 (Supporting information), compounds **1**–**6** showed a minimal inhibition toward SW620 and several common tumor cell lines with a cell inhibition rate of less than 10% even at 20 μmol/L. However, these compounds showed inhibition to the PTX-resistant cell SW620/AD300 under the condition of 1 μmol/L PTX. Assay demonstrated that substitution of different groups in sesterterpenoid altered the activity. Aromatic sesterterpenoids showed lower activity than other product, as evidenced by comparing **1** and **2** with **3**–**6**. The activity of compounds **3** and **4** suggested that the methoxy in C-5 can enhance the resensitization activity. Moreover, the disappearance of hydroxyl group at C-21 also enhance the activity, which supported by comparing **3** and **5** with **4** and **6**. Further research found that compound **4** significantly increased the sensitivity of SW620/AD300 cells to PTX, in which, the IC_{50} values of PTX without or with **4** in resistant SW620/AD300 cells were 1.79 μmol/L and 340 nmol/L, respectively, indicating a 5.26-fold depressed the resistance to PTX (Fig. 4A, Table S4 in Supporting information).

Inspired by the above interesting results, the effect of **4** alone or its combination with PTX on the cell proliferative and cell cycle potential of SW620/AD300 cells were examined using the colony formation assay and cell cycle analysis. **4** significantly enhanced the inhibitory activity of PTX on the colony formation of SW620/AD300 cells, stronger than that of **4** and PTX alone (Figs. 4B and C). Meanwhile, the cell cycle analysis showed that the combination of **4** and PTX significantly decreased the frequency of cells during G0/G1 phase but increased the frequency during G2/M (Figs. 4D and E), which was in accordance with the mechanism of PTX hampering mitosis.

Furthermore, the result of Rhodamine 123 accumulation assay exhibited that the higher dose of **4** added, the more intracellular Rho 123 percentage SW620/AD300 had (Figs. 4F and G), which indicated that **4** inhibitory the efflux function of P-gp. To reveal the possible binding model of **4** with P-gp, the molecular modeling was performed using the zosuquidar and human-mouse chimeric P-gp complex as the docking template (PDB code: 6FN1). The induced-fit docking-simulated best docking pose of **4** exhibited a docking score of −10.849 kcal/mol, indicating a relatively low binding free energy in complex with P-gp (Fig. S1 in Supporting information). **4** was mainly stabilized within the binding cavity in the transmembrane domain of P-gp, which is lined by residues ASN720, LEU723, TYR306, TYR309, PHE302, PHE727, PHE731, GLN837, PHE335, TRP231, SER978, PHE982, GLN989, MET985, GLN346, LEU64. Several hydrogen bonding interactions with the side chain of PHE302, TYR309, and GLN989 were also observed. In summary, **4** has the potential to be used in association with conventional chemotherapies in the treatment of cancers affected by P-gp-mediated multidrug resistance (MDR) relying on a considerable amount of favorable biological data.

In conclusion, six novel sesterterpenoids were isolated from endophytic fungus *Aspergillus nidulans*. Compounds **1**–**6** represent the first example of 5/5/5/5/6 pentacyclic ring skeleton, and compounds **1** and **2** were the first examples of aromatic pentacarbocyclic sesterterpenoids. Moreover, Compound **4** demonstrated potent resensitization of SW620/AD300 cells to PTX, which might be used in conventional chemotherapies in the treatment of cancers affected by P-gp-mediated MDR.

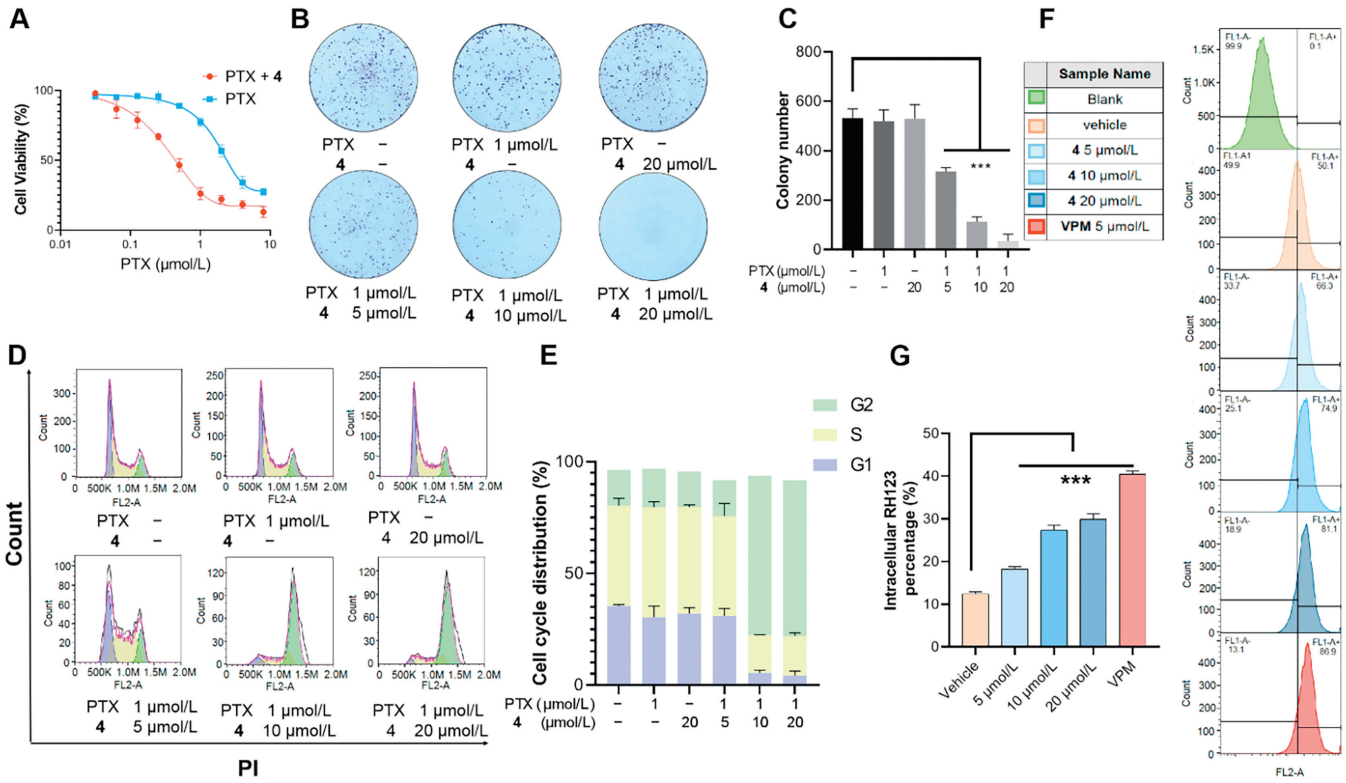

Fig. 4. Compound **4** effect the transport capacity of P-gp to reverse the PTX resistance of SW620/AD300 cells. (A) **4** significantly increased the inhibition effect of PTX to SW620/AD300 cells at 20 μmol/L. (B) The colony formation of SW620/AD300 cells after being treated with PTX, **4**, or their combination. (C) The colony number significantly decreased after being treated with the combination of **4** and PTX. (D) The cell cycle analysis of SW620/AD300 cells after being treated with PTX, **4**, or their combination. (E) The distribution of the cell cycle changed by the combination of **4** and PTX. (F) The fluorescence intensity of Rhodamine 123 in SW620/AD300 cells. (G) The Intracellular Rhodamine 123 percentage with 30 min was treated by 5, 10, 20 μmol/L of **4**. Data are presented as the mean ± standard deviation (SD), n=3. $^{***}P < 0.001$ *vs.* negative control (NC).

Declaration of competing interest

The authors declare that they have no known competing financial interests or personal relationships that could have appeared to influence the work reported in this paper.

Acknowledgments

This work This work was financially supported by the National Key Research and Development Program of China (No. 2021YFA0910500), the National Natural Science Foundation of China (Nos. U22A20380, 82104028, 82173706 and 82373755), Innovative Research Groups of the National Natural Science Foundation of China (No. 81721005), the Science and Technology Major Project of Hubei Province (No. 2021ACA012), the Fundamental Research Funds for the Central Universities, HUST (No. 2021JYCXJJ058). We thank the Analytical and Testing Center at Huazhong University of Science and Technology for assistance in the acquisition of the ECD, UV, and IR spectra.

Supplementary materials

Supplementary material associated with this article can be found, in the online version, at doi:10.1016/j.cclet.2023.109100.

References

[1] J.R. Hanson, Nat. Prod. Rep. 3 (1986) 123–132.
[2] J.R. Hanson, Nat. Prod. Rep. 9 (1992) 481–489.
[3] J.R. Hanson, Nat. Prod. Rep. 13 (1996) 529–535.
[4] Y. Liu, L. Wang, J.H. Jung, S. Zhang, Nat. Prod. Rep. 24 (2007) 1401–1429.
[5] L. Wang, B. Yang, X.P. Lin, X.F. Zhou, Y. Liu, Nat. Prod. Rep. 30 (2013) 455–473.
[6] K. Li, K.R. Gustafson, Nat. Prod. Rep. 38 (2021) 1251–1281.
[7] R. Jain, J. Am. Chem. Soc. 46 (2009) 243–244.
[8] M. Schumacher, T. Juncker, M. Schnekenburger, F. Gaascht, M. Diederich, Genes Nutr. 6 (2011) 89–92.
[9] A. García, V. Bocanegra García, J.P. Palma Nicolás, G. Rivera, Eur. J. Med. Chem. 49 (2012) 1–23.
[10] F. Baquero, M. Coque Teresa, F. de la Cruz, Antimicrob. Agents Chemother. 55 (2011) 3649–3660.
[11] D. Li, M. Yang, R. Mu, et al., Chin. Chem. Lett. 34 (2023) 10746.
[12] W. Wang, Y. Lee, T.G. Lee, et al., Org. Lett. 14 (2012) 4486–4489.
[13] K. Guo, Y. Liu, S.H. Li, Nat. Prod. Rep. 38 (2021) 2293–2314.
[14] S.J. Piao, W.H. Jiao, F. Yang, et al., Mar. Drugs 12 (2014) 4096–4109.
[15] M. Wang, A. Sciorillo, S. Read, et al., J. Nat. Prod. 85 (2022) 1274–1281.
[16] J.K. Woo, C.K. Kim, C.H. Ahn, et al., J. Nat. Prod. 78 (2015) 218–224.
[17] Q.M. Li, J.G. Luo, H.J. Zhao, et al., Asian J. Org. Chem. 4 (2015) 1366–1369.
[18] S. Chen, H. Liu, S. Li, et al., Chin. Chem. Lett. 34 (2023) 107513.
[19] S. Lin, J. Huang, H. Zeng, et al., Chin. Chem. Lett. 33 (2022) 4587–4594.
[20] M. Zhang, S. Yan, Y. Liang, et al., Org. Chem. Front 7 (2020) 3486–3492.
[21] P. Zhou, X. Zhang, C. Dai, et al., J. Org. Chem. 87 (2022) 7333–7341.
[22] J.W. Tang, L.M. Kong, W.Y. Zu, et al., Org. Lett. 21 (2019) 771–775.
[23] Q. Li, C.M. Chen, M.S. Wei, et al., Org. Lett. 21 (2019) 2290–2293.
[24] M. Okada, Y. Matsuda, T. Mitsuhashi, et al., J. Am. Chem. Soc. 138 (2016) 10011–10018.
[25] H. Sato, T. Mitsuhashi, M. Yamazaki, I. Abe, M. Uchiyama, Angew. Chem. Int. Ed. 57 (2018) 14752–14757.
[26] B. Yang, W. Sun, J. Wang, et al., Mar. Drugs 16 (2018) 110.